NASA TECHNICAL NOTE

NASA TN D-8504

ELASTIC DISTORTION OF FLANGED INNER RING OF HIGH-SPEED CYLINDRICAL ROLLER BEARING

Christopher M. Taylor

Lewis Research Center

Cleveland, Ohio 44135

NATIONAL AERONAUTICS AND SPACE ADMINISTRATION • WASHINGTON, D. C. • JUNE 1977

1. Report No.	2. Government Accession No.	3. Recipient's Catalog No.
NASA TN D-8504		

4. Title and Subtitle	5. Report Date
ELASTIC DISTORTION OF FLANGED INNER RING OF HIGH-SPEED CYLINDRICAL ROLLER BEARING	June 1977
	6. Performing Organization Code
7. Author(s)	8. Performing Organization Report No.
Christopher M. Taylor	E-9054
	10. Work Unit No.
9. Performing Organization Name and Address	505-04
Lewis Research Center National Aeronautics and Space Administration Cleveland, Ohio 44135	11. Contract or Grant No.
	13. Type of Report and Period Covered
12. Sponsoring Agency Name and Address	Technical Note
National Aeronautics and Space Administration Washington, D.C. 20546	14. Sponsoring Agency Code

15. Supplementary Notes

16. Abstract

The elastic distortion of the inner ring of an experimental 3×10^6 DN roller bearing is investigated analytically. The geometry of the experimental bearing is unusually complex, and for this reason a bearing with an axially symmetric inner ring is also analyzed. Only the inner ring and shaft are considered using a two-dimensional finite-element program that can accommodate interference between these components. The results suggest that the elastic distortions are modest in relation to the design clearances associated with the experimental bearing. The variation of the radial deflection of the raceway may, however, be significant in some circumstances.

17. Key Words (Suggested by Author(s))	18. Distribution Statement
Bearing Roller Distortion Finite-element method	Unclassified - unlimited STAR Category 37

19. Security Classif. (of this report)	20. Security Classif. (of this page)	21. No. of Pages	22. Price*
Unclassified	Unclassified	17	A02

* For sale by the National Technical Information Service, Springfield, Virginia 22161

ELASTIC DISTORTION OF FLANGED INNER RING OF HIGH-SPEED CYLINDRICAL ROLLER BEARING

by Christopher M. Taylor*

Lewis Research Center

SUMMARY

A finite-element computer program is used to analyze the elastic distortions occurring in the inner ring of an experimental 3×10^6 DN roller bearing. The inner ring and shaft system is examined, these components having a relative interference. The computer program employed was developed to enable direct analysis of situations in which such an interference occurs. The geometry of the bearing being tested is unusually complex, thus a more conventional symmetric inner ring on a uniformly hollow shaft is also studied.

All loading on the inner ring and shaft was taken as axisymmetric. The results presented include raceway and flange distortions as a function of shaft rotational speed. The character of these distortions is related to the interference pressure between the shaft and inner ring, which is also detailed. The magnitude of the dominant stress, the hoop stress, near the raceway is also presented.

The results indicated that the elastic distortions of the inner ring of the experimental bearing are modest in relation to the important clearances. Thus, the radial internal clearance is considered to be entirely adequate and "pinching" of the rollers by the flanges should not occur. The variation of the radial deflection of the raceway of the inner ring suggests that at some operating conditions it may have a significant effect. For example, a maximum variation of raceway radius of about 2.6 micrometer is predicted at zero shaft speed. This is sizeable in relation to typical tolerances on track taper. Partial separation of the inner ring from the shaft is predicted to occur at about 17 000 rpm; however, no consideration was given in the analysis to the ring retention device used in practice. It is estimated that an interference 2.4 times that used would be required to prevent any separation of inner ring and shaft at a rotational speed of 25 500 rpm (about 3×10^6 DN).

*Lecturer in Mechanical Engineering, University of Leeds, Leeds, England; National Research Council - National Aeronautics and Space Administration Senior Research Associate at the Lewis Research Center in 1976-1977.

INTRODUCTION

The requirement for the mainshaft bearings of large gas-turbine engines to operate at DN values of 3×10^6 by the 1980's has been laid down for several years. The implementation of successful designs for such bearings will represent a significant advance in rolling-element bearing technology compared with the state-of-the-art at the commencement of the current decade.

Much attention has already been paid to the problems consequent to the operation of rolling bearings at DN values of the order mentioned (e.g., ref. 1). Research has provided answers to lubrication and heat removal problems, and the improvements in the fatigue life capability of bearing steels have offset the more arduous loading conditions due to centrifugal effects.

The work presented here is intended to compliment a current experimental and theoretical examination of advanced cylindrical-element roller bearings. Studies of roller bearings for the next generation of gas turbines have lagged behind those of ball bearings; however, evidence of problems in their operation has stimulated closer attention. The prime purpose of the study reported was to estimate distortions for a design of high-speed cylindrical roller bearing undergoing experimental testing.

Because of the large centrifugal forces that occur in the roller bearings being studied, a substantial interference must exist between the shaft and inner ring under zero speed conditions. The interference pressure at the shaft and inner ring interface will be important in the determination of the ring distortion, and detailed account of it must be taken. It is a somewhat cumbersome, if straightforward, matter to use conventional finite-element programs to determine interference pressure distributions and, subsequently, component distortions and stresses. To circumnavigate this inconvenience, a computer program for axisymmetrically loaded components has been developed whereby a direct solution for the elastic distortion of parts having relative interference can be obtained. The program has been described elsewhere (ref. 2) and enables axially varying deflections to be determined. In general, when the elastic distortion of rolling-element bearings has been examined, axially invariant as well as axisymmetric conditions have been taken to apply.

The experiments on high-speed roller bearings being conducted at NASA Lewis Research Center (and as yet undocumented) deal with a rotating inner ring situation, in which the fixed flanges to locate the rollers axially are on this inner ring. Since the distortions of the inner ring were, therefore, the major interest, it was decided to examine only the inner ring and shaft system. For high-speed applications the rolling-element load at the outer ring may be substantially higher than at the inner ring contact. Indeed, the centrifugal loading on a rolling element may be such as to unload the inner ring contact. Thus, it was considered a reasonable approximation to neglect the effect of roller loads on the distortion of the inner-ring and shaft system.

RESULTS AND DISCUSSION

General

In figure 1 the inner ring and shaft of a bearing currently being tested are shown. The configuration has been modified slightly to facilitate the finite-element modeling; for example, corner radii have been omitted. The geometry of the test bearing inner ring and its shaft is unusually complex. It was felt that some general points relating to the type of analysis undertaken might be masked by the consideration of this situation alone. Therefore, an alternative, symmetrical, and simpler geometry was also considered (fig. 2). Setting aside the puller groove of the test bearing, the inner ring geometry of the bearing in figure 2 is very similar. For convenience the two cases will be referred to as the "symmetrical bearing" and the "test bearing."

The Symmetrical Bearing

The geometry of figure 2 was modeled using purely rectangular finite elements. The distortions and stresses in the inner ring and shaft were investigated for the following conditions using the computer program described in reference 2: Shaft rotational speeds, 0, 5000, 10 000, 15 000, 20 000, 25 000, 30 000 rpm; and radial interference between the shaft and inner ring, 5.08×10^{-5} meter. For both the symmetrical and test bearings, the shaft and ring were taken to be composed of the same steel having the following properties: Young's modulus, 2.07×10^{11} pascals; Poisson's ratio, 0.3; density, 7480 kilograms per cubic meter. The axisymmetric loading on the system comprised only inertial and interference loads. As has been mentioned already, rolling-element loads were not considered, and for the analyses conducted no thermal loading was applied.

It is appropriate here to comment on the frictional conditions that may pertain axially in the region of contact between the shaft and inner ring. In the computer program (ref. 2), matching nodes in the finite-element mesh are set up on the components having interference; that is, for the case in question, each node on the shaft in the region of interference has a corresponding node on the inner ring at the same spacial position. These corresponding nodes are related radially according to the interference condition specified. The problem arises as to what relative movement in the axial direction (a minute slip) should be permitted between corresponding nodes. Three possibilities are apparent and can be applied in the computer program:

(1) Corresponding or matching nodes can be restrained to have no relative axial movement (i.e., have axial interference). In this situation, with complete surface adhesion, a surface traction is present at the inner ring and shaft interface.

(2) Corresponding or matching nodes can be allowed to move freely axially (i.e., slip). For this case the inner-ring and shaft interface transmits no shear, the contact being frictionless.

(3) Corresponding or matching nodes can be allowed to move freely relative to each other if the ratio of axial to radial force at them exceeds some critical value (the coefficient of friction).

The third option was chosen for the current work, a coefficient of friction of 0.5 being taken to apply at the steel-steel, inner ring - shaft contact. Further comment on this aspect will be made later.

Details of the results presented will now be given. At a shaft rotational speed of 30 000 rpm the computer program indicated that the radial interference between the shaft and inner ring had been partially lost at the outer edge of the ring. Under these circumstances the operation of the program is automatically terminated. Hence, the results presented are for a maximum shaft rotational speed of 25 000 rpm.

Figure 2 may be referred to for the coordinate system used and the sign convention adopted. The notation U is used for deflection. Thus, $(U_Z)_2$ is the movement in the Z direction of point 2 and $(U_R)_2 - (U_R)_3$ is the difference in radial deflections of the points 2 and 3. The term "rake" will be used to mean the difference in axial deflection between the extreme points (1 and 2) of the flange thrust face. Thus, the flange rake is $(U_Z)_1 - (U_Z)_2$.

The distribution of interference pressure along the region of contact between the inner ring and shaft (the outer edge of the ring being at the left-hand side) shown in figure 3 demonstrates the substantial rise in pressure at the outer edge of the ring due to the stiffening effect of the shafting outside the projected bearing area. The solid lines of figure 3 relate to the condition for axial slip at the interference location, based on a coefficient of friction of 0.5. At zero shaft rotational speed, the forces developed at the interferring nodes were such that no axial slip took place at any station. The dashed line in figure 3(a) (zero shaft speed case) indicates the distribution of interference pressure obtained if the contacting surfaces were taken to be frictionless in the axial direction.

At a shaft rotational speed of 25 000 rpm, all the nodal stations in the region of interference suffered slip, the ratio of axial to radial force having exceeded 0.5 at each. The difference in interference pressure, particularly at the outer edge of the ring if no slip is permitted, is shown by the dashed line. This effect has been noted by others (ref. 3).

For the intermediate shaft rotational speed considered, the nodes near the outer edge of the ring had slipped, whereas those nearer the center of the ring still remained locked together axially. This partial slip manifests itself in the increased interference pressure at the outer edge compared with the zero rotational speed curve.

Although the rise in interference pressure only occurs over a small axial distance, it can be substantial, and in some cases its effects could be significant (e.g., in flange distortion).

The hoop or circumferential stress (tensile) in the inner ring was much greater than the radial and axial stresses. The variation of hoop stress through the depth of the ring was not great, as would be expected, and its mean value close to the raceway (at the center of the elements bordering the raceway) is plotted as a function of rotational speed in figure 4. The variation of this hoop stress along the length of the raceway does not exceed 2.5 percent. Stresses of the magnitude indicated (250 MPa) might be influential in the propagation of a fatigue crack once it has been initiated.

Figures 5 and 6 present information relating to the elastic distortion of the inner-ring flanges. Figure 5 shows that the magnitude of the slope or rake of the flange faces at the raceway edges is small, typically of the order of one-half of a micrometer. It has been assumed that before the inner ring is mounted on the shaft these flange faces are perpendicular to the raceway. Intuitively, it might be expected that the rake, as defined, would increase with increasing rotational speed as the inertial effect on the flanges came more into play. The fact that it does not is explained by the dominance of the distortions due to the interference pressure as compared with the effect of centrifugal forces. Thus, as can be seen in figure 3, the interference pressure falls substantially at higher speeds, and this fall has a major effect on the flange movement.

The axial contraction of the distance between the flange thrust face tips increases with speed and, as can be inferred from figure 6, is about 8 micrometers ($2 \times (U_Z)_1$) at a shaft speed of 23 000 rpm. The primary influence causing this contraction is what might be called the Poisson effect due to centrifugal forces; that is, as the ring is expanded to a larger mean radius, it contracts axially.

The mean value of the radial deflection of the raceway as a function of shaft rotational speed is shown in figure 7. This deflection is of interest in the calculation of the operating radial internal clearance. The maximum raceway radial deflection occurs at the intersection with the flanges and the minimum at the center of the raceway. As can be seen from figure 8, the difference of radial deflection along the raceway is about 0.7 micrometer at a shaft speed of 10 000 rpm. This figure is of interest in relation to current practice of specifying raceway flatness at manufacture of very-high-speed roller bearings not to exceed about 0.5 micrometer.

The Test Bearing

The results of the analysis for the bearing undergoing experimental testing (as represented in fig. 1) will now be presented and discussed. The conditions investigated

were - shaft rotational speed, 0, 5000, 10 000, 15 000, and 17 000 rpm and radial interference between the inner ring and shaft, 3.556×10^{-5} meter.

As can be seen, the assembly interference for the test bearing is 30 percent less than that considered for the symmetrical bearing case already dealt with. The analysis indicated that a partial loss of interference occurred at a rotational speed just below 17 000 rpm. This took place at the left-hand edge of the inner ring. (See fig. 1.) A partial loss of interference does not infer that the bearing will suffer any distress, and it is interesting to note that speeds exceeding 17 000 rpm have already been successfully employed in the experimental program. It is also pertinent to mention that no account was taken of the ring axial retention device used in practice. The approximate location of this retention device is shown in figure 1, but the finite-element analysis took no account of it. The results presented, therefore, are limited to speeds less than 17 000 rpm. Once again axial slip at the ring and shaft interface was permitted if the coefficient of friction at a node location exceeded 0.5.

With the particular inner ring and shaft geometry of the test bearing, it can be seen from figure 9 how difficult it would be to undertake meaningful simplified calculations as regards the interference pressure developed and its detailed effects. At either end of the inner ring the sharp rise in interference pressure consequent mainly on the stiffness of the shafting outside the bearing region is apparent. However, the distribution of the interference pressure axially could not be predicted by simple calculations. Hence, an estimation of, say, the raceway radial deflection by a simplified method would be brought into question. At zero rotational speed, although the maximum interference pressure occurs at the left-hand edge of the inner ring, it drops sharply as the ring is traversed towards the right-hand edge. The interference pressure then builds up, moving farther in the axial direction, the location of the center of pressure of the distribution certainly being nearer the right-hand edge of the ring.

Although the double reversal of the slopes of two of the interference pressure distributions near the right-hand edge of the inner ring is probably a "real" effect, the same phenomenon at the left-hand edge may well be a consequence of the numerical analysis technique used to determine the pressure distribution. It was assumed that the pressure varied linearly between nodes in the interference region and that a significant change in radial interference force from one node to another can result in this effect, which has been obtained by others (ref. 3). It should be emphasized that the overall interference pressure distribution will be reliably reflected by the analysis.

It can be seen from figure 9 that the effect of increasing the shaft rotational speed is to tend to flatten the pressure distribution in the central portion. Certain features of the elastic distortion of the inner ring reflect this predicted variation in interference pressure. The reason for the nature of the interference pressure distributions is related primarily to the location of the ring on the shaft with respect to the annular hole in the latter.

The variation with speed of hoop stress near the raceway is shown in figure 10. As with the symmetrical bearing, the variation of hoop stress along the raceway is small. The overall level of the hoop stress is somewhat lower than for the symmetrical bearing due to the lower radial interference adopted. Figure 11 details the amount by which the flange tips (points A and D, fig. 1) approach each other, this being a measure of the tendency to "pinch" the rollers. The approach is slightly less than 5 micrometers for the worst case. Since the unmounted inner ring of the experimental bearing gave an axial roller clearance of about 40 micrometers between flanges, the elastic distortion of the flanges should not prove of importance. The approach of the flanges decreases with increasing rotational speed. This behavior is contrary to that obtained for the symmetrical bearing. The explanation of this appears to lie in the variation of the distribution of the interference pressure and its effects, including the elastic distortion of the flanges.

In figure 12 the rake of the bearing flanges at the raceway edges is detailed as a function of shaft rotational speed. It is particularly noticeable that at zero rotational speed the point D (fig. 1) is to the left of point C. Relative to point C, the point D moves clockwise as the speed is increased, eventually moving to the right of C. This behavior is consistent with the variation of interference pressure shown in figure 9 and goes a long way to explaining the trends of the curve of figure 11.

Figure 13 shows the mean value of raceway radial deflection as a function of shaft rotational speed. At 15 000 rpm the mean deflection of the raceway radially is just less than 40 micrometers. The design unmounted radial internal clearance of the test bearing is 125 micrometers. Keeping in mind other influences on the operating internal clearance, the unmounted clearance should be entirely adequate.

The maximum difference of raceway radial deflection along its length is plotted as a function of shaft speed in figure 14. At zero rotational speed there is a maximum difference in radial deflection of the raceway of some 2.6 micrometers. It could be correctly inferred from the interference pressure distribution of figure 9 that the maximum radial deflection of the raceway at zero shaft speed occurs at the puller groove end of the inner ring, whereas, the smallest radial deflection is at, or close to, the left-hand edge of the raceway. As the rotational speed is increased, the changing interference pressure reduces this maximum difference in radial deflection until at about 13 000 rpm the raceway becomes approximately parallel to the rotational axis. A further increase in shaft speed causes the raceway to "tilt" in the opposite direction. Profiles of the raceway relative to the rotational axis are shown for three shaft speeds in figure 15. In this figure the ring flanges and puller groove are shown dashed, undistorted, and not to scale, in order to relate their position to the raceway profiles. The variation of the radial deflection of the raceway along its length is substantial for some shaft rotational speeds. The variation may be significant as regards the bearing performance; however, it is difficult to postulate with any certainty what its effects might be.

CONCLUDING REMARKS

The analysis of the test bearing inner-ring and shaft geometry has indicated that a separation of the inner ring and shaft occurs at the left-hand edge of the ring at a shaft rotational speed of about 17 000 rpm. This speed is less than the contemplated maximum speed of operation; however, this observation need not have practical implications, particularly when it is recalled that an inner ring retention device (fig. 1), not considered in the analysis, is employed in practice. However, the point still emphasizes the fact that simple calculations of shaft rotational speed at which interference between the inner ring and shaft is lost can be in error where complex geometries are involved. The design interference employed should of itself be sufficient to prevent separation, with any inner-ring retention device providing extra confidence.

Results for the distortion of the test bearing inner ring beyond a shaft speed of 17 000 rpm have not been presented, because of an uncertainty about the uniqueness of solutions when radial separation has occurred at some location. However, the radial interference between the inner ring and shaft to insure that no separation would occur at a rotational speed of 25 500 rpm (about 3×10^6 DN) was determined to be 8.636×10^{-5} meter. This is some 2.4 times greater than the radial interference actually used.

The method of analysis used in this report (ref. 2) might be useful for a number of investigations; for example,

(1) The optimization of shaft geometry and bearing location to minimize any adverse effects of elastic distortion. In the test bearing application the location of the bearing with respect to the annulus in the shaft influences some distortion effects considerably.

(2) The study of the design and effect of ring retention devices.

(3) The evaluation of appropriate, premachined flange-thrust-face angles.

(4) The determination of flange distortions, which may be important to the ability of cylindrical rollers bearings to carry substantial thrust loads under some circumstances.

SUMMARY OF RESULTS

Symmetrical Bearing

The analysis of the symmetrical bearing demonstrated three main points for the geometry in question:

1. The dominance of the Poisson effect in the relative axial movement of the flanges

2. The importance of the interference pressure, vis-vis the inertial forces, in determining the flange rake.

3. The influence of the frictional boundary conditions on the interference pressure distribution, particularly at high shaft speeds at the axial extremities of the inner ring.

Test Bearing

It is concluded from the analysis of the test bearing that elastic distortions of the inner ring are modest in relationship to the design clearances of the bearing. However, the variation of the radial deflection of the raceway appears to be significantly high for some operating conditions. The main results of the analysis are

1. Partial separation of the inner ring from the shaft is predicted at a shaft rotational speed just less than 17 000 rpm.

2. A radial interference 2.4 times that actually used would be needed to avoid any ring and shaft separation at a 3×10^6 DN operating condition.

3. The maximum approach of the tips of the inner-ring flanges is just less than 5 micrometers at zero shaft speed and decreases with increasing speed.

4. The mean radial deflection of the raceway is just less than 40 micrometers at a rotational speed of 15 000 rpm.

5. The maximum difference in raceway radial deflection at zero shaft rotational speed is about 2.6 micrometers.

6. Near the raceway of the inner ring, a hoop stress of 1.2×10^8 pascals is predicted at a rotational speed of 15 000 rpm.

Lewis Research Center,
National Aeronautics and Space Administration,
Cleveland, Ohio, March 30, 1977,
505-04.

REFERENCES

1. Bamberger, E. N.; Zaretsky, E. V.; and Signer, H.: Endurance and Failure Characteristic of Main-Shaft Jet Engine Bearing at 3×10^6 DN. J. Lubri. Tech., vol. 98, no. 4, Oct. 1976, pp. 580-585.

2. Taylor, C. M.: Finite-Element Computer Program for Axisymmetric Loading Situations Where Components May Have a Relative Interference Fit. NASA TN D-8483, 1977.

3. Wilson, E. A.; and Parsons, B.: Finite Element Analysis of Elastic Contact Problems Using Differential Displacements. Int. J. Num. Methods Eng., vol. 2, no. 3, July-Sept. 1970, pp. 387-395.

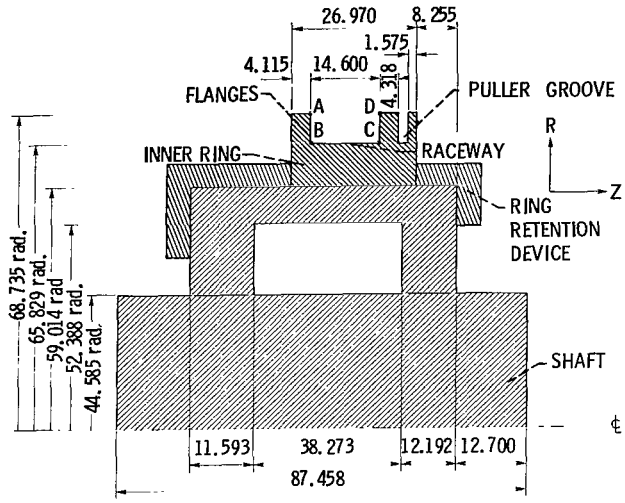

Figure 1. - The test bearing inner ring and shaft assembly. (Dimensions are in mm.)

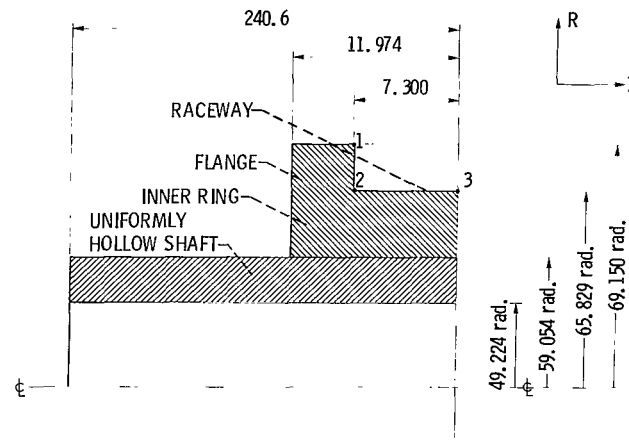

Figure 2. - Half-section of symmetrical bearing inner ring and shaft assembly. (Dimensions are in mm.)

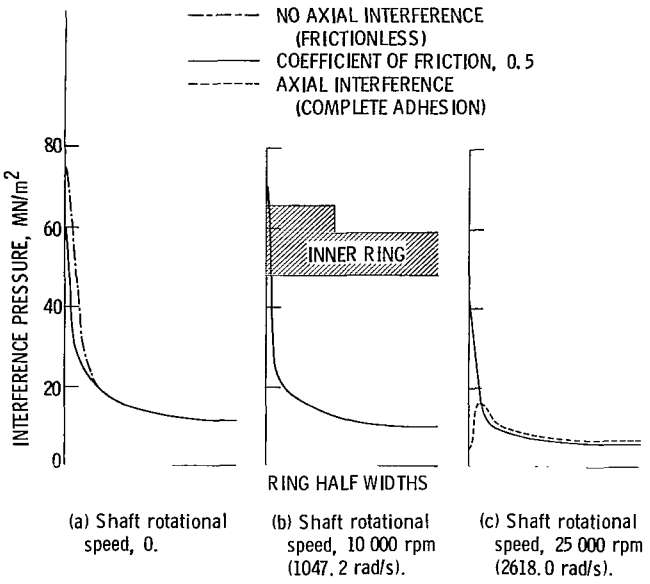

Figure 3. - Distribution of radial interference pressure at ring and shaft interface for three shaft rotational speeds (symmetrical bearing).

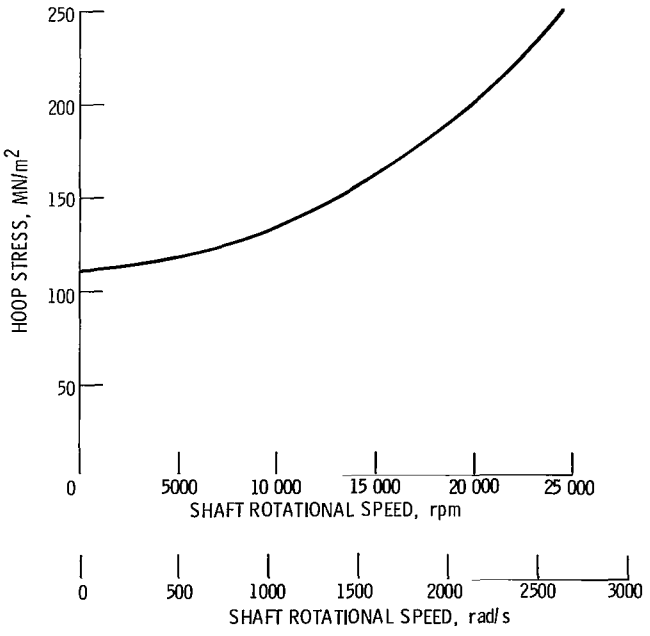

Figure 4. - Hoop stress near raceway as function of shaft rotational speed (symmetrical bearing).

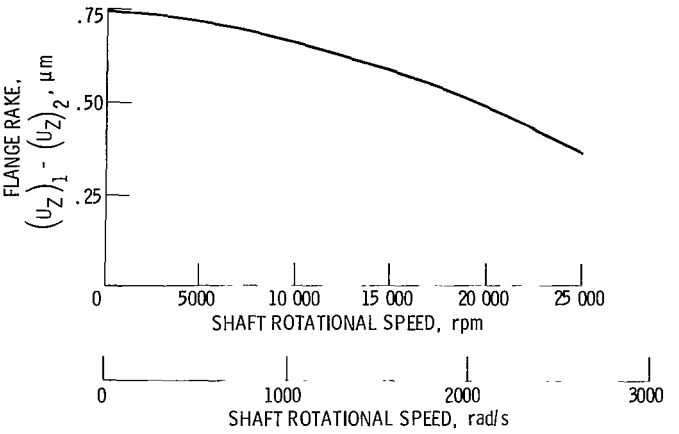

Figure 5. - Flange rake as function of shaft rotational speed (symmetrical bearing).

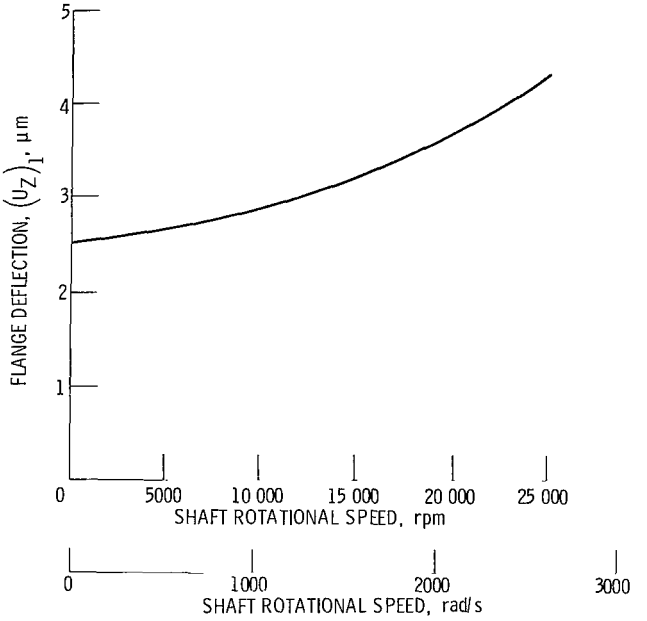

Figure 6. - Flange deflection at point 1 as function of rotational speed (symmetrical bearing).

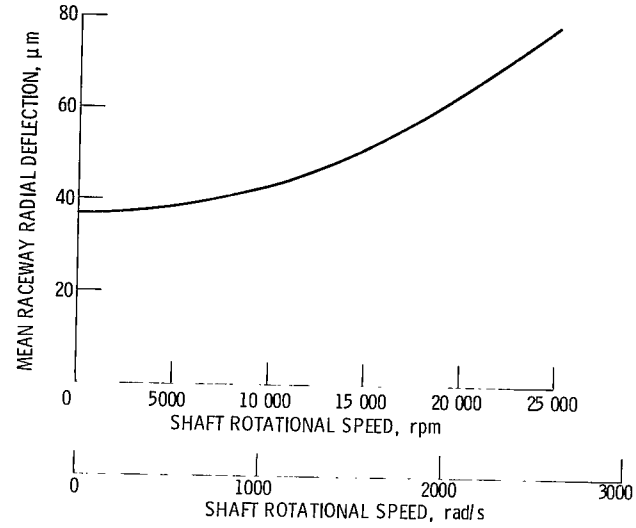

Figure 7. - Mean raceway radial deflection as function of shaft rotational speed (symmetrical bearing).

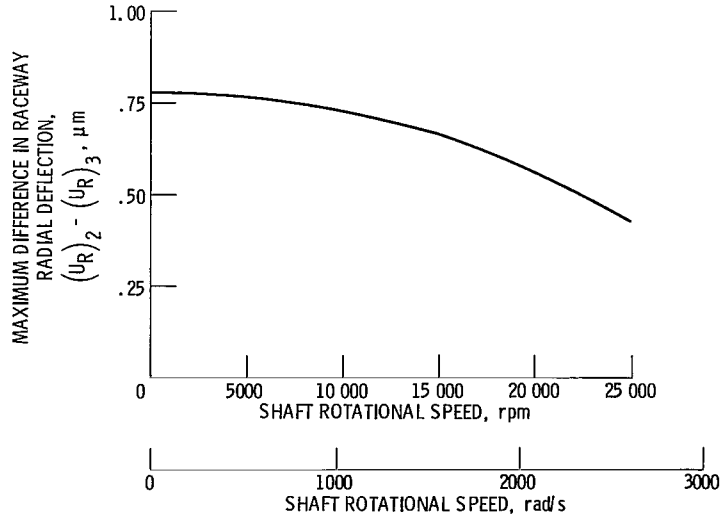

Figure 8. - Maximum difference in raceway radial deflection as function of shaft rotational speed (symmetrical bearing).

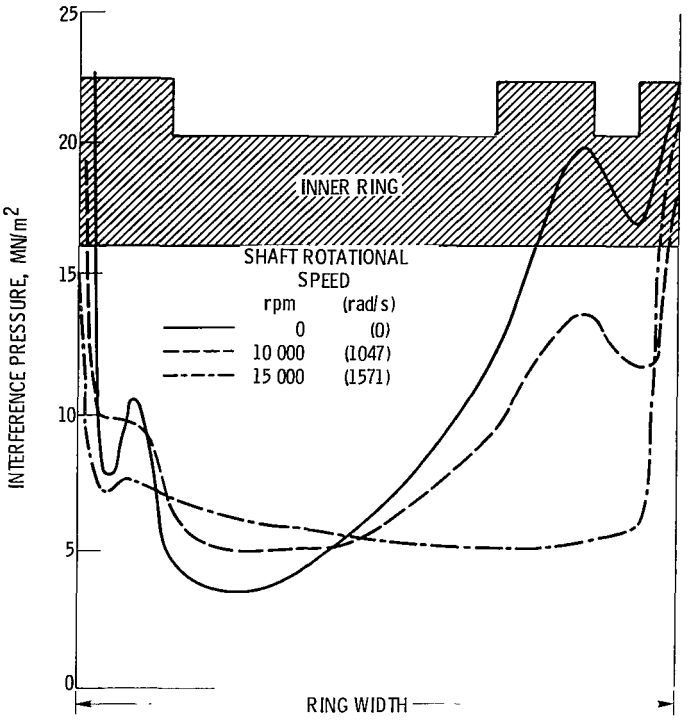

Figure 9. - Distribution of radial interference pressure at ring and shaft interface for three shaft rotational speeds (test bearing).

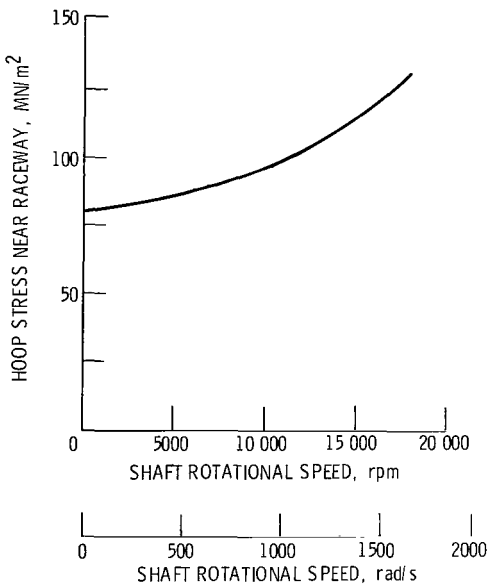

Figure 10. - Hoop stress near raceway as function of shaft rotational speed (test bearing).

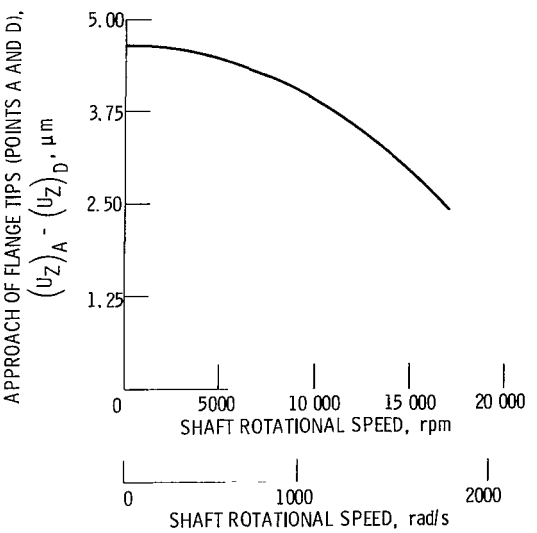

Figure 11. - Approach of flange tips (points A and D) as function of shaft rotational speed (test bearing).

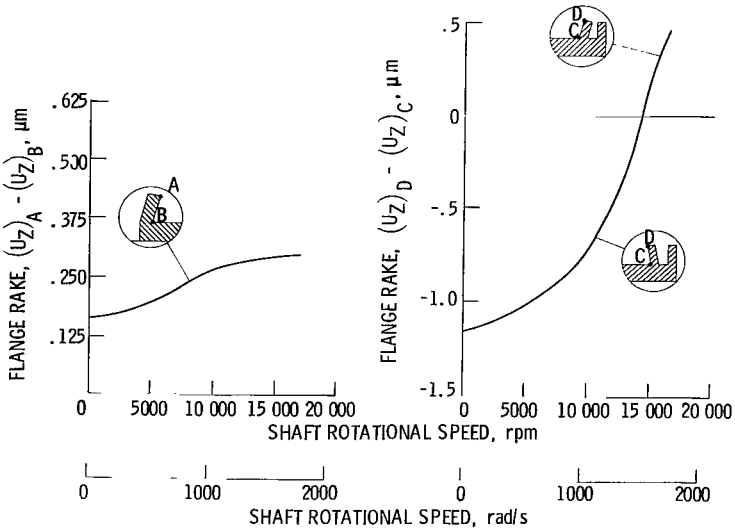

Figure 12. - Flange rakes as function of shaft rotational speed (test bearing).

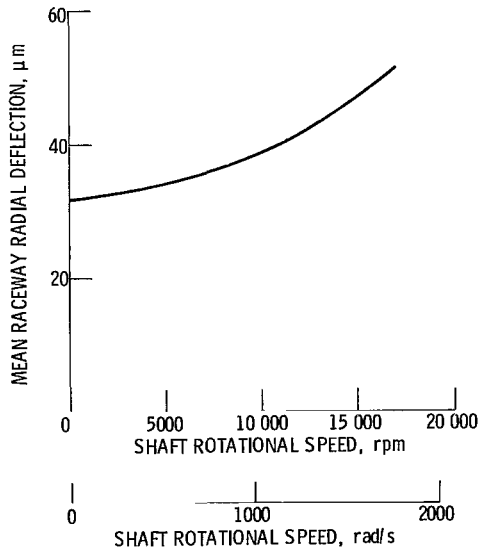

Figure 13. - Mean raceway radial deflection as function of shaft rotational speed (test bearing).

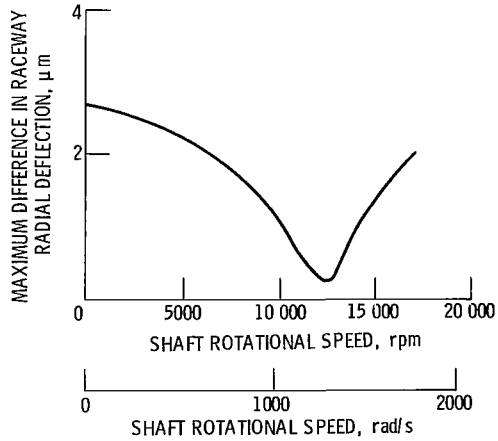

Figure 14. - Maximum difference in raceway radial deflection as function of shaft rotational speed (test bearing).

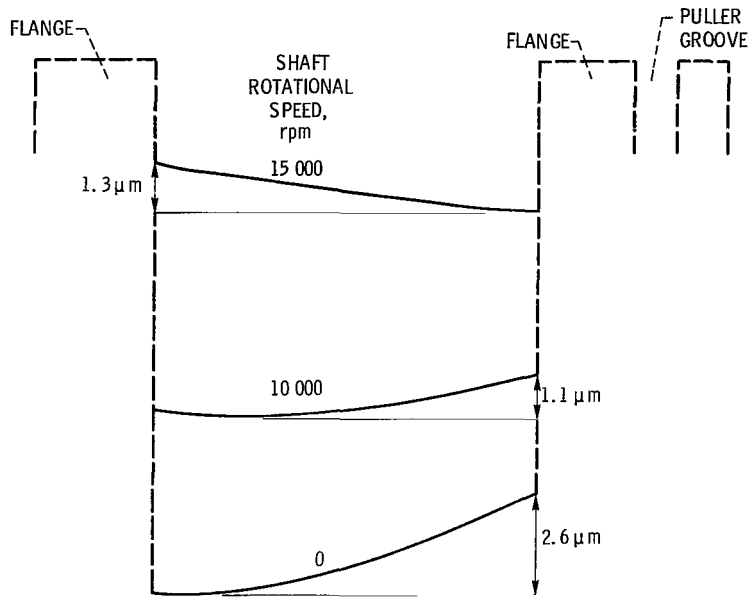

Figure 15. - Raceway profiles relative to rotational axis for three shaft speeds (test bearing).

NATIONAL AERONAUTICS AND SPACE ADMINISTRATION
WASHINGTON, D.C. 20546

OFFICIAL BUSINESS
PENALTY FOR PRIVATE USE $300

SPECIAL FOURTH-CLASS RATE BOOK

POSTAGE AND FEES PAID
NATIONAL AERONAUTICS AND SPACE ADMINISTRATION
451

U.S.MAIL

389 001 C1 U D 770527 S00903DS
DEPT OF THE AIR FORCE
AF WEAPONS LABORATORY
ATTN: TECHNICAL LIBRARY (SUL)
KIRTLAND AFB NM 87117

POSTMASTER: If Undeliverable (Section 158 Postal Manual) Do Not Return

"The aeronautical and space activities of the United States shall be conducted so as to contribute . . . to the expansion of human knowledge of phenomena in the atmosphere and space. The Administration shall provide for the widest practicable and appropriate dissemination of information concerning its activities and the results thereof."

—NATIONAL AERONAUTICS AND SPACE ACT OF 1958

NASA SCIENTIFIC AND TECHNICAL PUBLICATIONS

TECHNICAL REPORTS: Scientific and technical information considered important, complete, and a lasting contribution to existing knowledge.

TECHNICAL NOTES: Information less broad in scope but nevertheless of importance as a contribution to existing knowledge.

TECHNICAL MEMORANDUMS: Information receiving limited distribution because of preliminary data, security classification, or other reasons. Also includes conference proceedings with either limited or unlimited distribution.

CONTRACTOR REPORTS: Scientific and technical information generated under a NASA contract or grant and considered an important contribution to existing knowledge.

TECHNICAL TRANSLATIONS: Information published in a foreign language considered to merit NASA distribution in English.

SPECIAL PUBLICATIONS: Information derived from or of value to NASA activities. Publications include final reports of major projects, monographs, data compilations, handbooks, sourcebooks, and special bibliographies.

TECHNOLOGY UTILIZATION PUBLICATIONS: Information on technology used by NASA that may be of particular interest in commercial and other non-aerospace applications. Publications include Tech Briefs, Technology Utilization Reports and Technology Surveys.

Details on the availability of these publications may be obtained from:

SCIENTIFIC AND TECHNICAL INFORMATION OFFICE

NATIONAL AERONAUTICS AND SPACE ADMINISTRATION

Washington, D.C. 20546